Transient Loss of Voltage Control of Ca^{2+} Release in the Presence of Maurocalcine in Skeletal Muscle

Sandrine Pouvreau,* Laszlo Csernoch,† Bruno Allard,* Jean Marc Sabatier,‡ Michel De Waard,§ Michel Ronjat,§ and Vincent Jacquemond*

*Physiologie Intégrative Cellulaire et Moléculaire, Université Claude Bernard Lyon 1, UMR CNRS 5123, 69622 Villeurbanne, France; †Department of Physiology, Medical and Health Science Center, University of Debrecen, Debrecen H-4012, Hungary; ‡ERT 62, Université de la Méditerranée–Ambrilia Biopharma S.A., Faculté de Médecine Nord, 13916 Marseille, France; and §INSERM U607/DRDC, CEA, 38054 Grenoble, France

ABSTRACT In skeletal muscle, sarcoplasmic reticulum (SR) calcium release is controlled by the plasma membrane voltage through interactions between the voltage-sensing dihydropyridine receptor (DHPr) and the ryanodine receptor (RYr) calcium release channel. Maurocalcine (MCa), a scorpion toxin peptide presenting some homology with a segment of a cytoplasmic loop of the DHPr, has been previously shown to strongly affect the activity of the isolated RYr. We injected MCa into mouse skeletal muscle fibers and measured intracellular calcium under voltage-clamp conditions. Voltage-activated calcium transients exhibited similar properties in control and in MCa-injected fibers during the depolarizing pulses, and the voltage dependence of calcium release was similar under the two conditions. However, MCa was responsible for a pronounced sustained phase of Ca^{2+} elevation that proceeded for seconds following membrane repolarization, with no concurrent alteration of the membrane current. The magnitude of the underlying uncontrolled extra phase of Ca^{2+} release correlated well with the peak calcium release during the pulse. Results suggest that MCa binds to RYr that open on membrane depolarization and that this interaction specifically alters the process of repolarization-induced closure of the channels.

INTRODUCTION

Optimal control of voluntary movement and force production relies ultimately on the efficacy of excitation-contraction (e-c) coupling of skeletal muscle. The contraction of a skeletal muscle fiber is rapidly initiated and stopped by changes in the voltage across the plasma membrane, physiologically an action potential or a train of action potentials. The coupling between membrane depolarization and the resulting transient rise in cytoplasmic [Ca^{2+}] that activates the contractile machinery is ensured by two types of ion channel proteins facing each other across an ~15-nm-wide gap at the triadic junction; these two are the DHPr in the plasma/transverse-tubule membrane, which senses the changes in voltage, and the RYr calcium release channel in the SR membrane. The opening and closure of the RYr calcium channel are subordinated to voltage-dependent conformational changes of the DHPr, but the details of the functional interactions between the two still remain obscure. Since the early 1990s, several lines of evidence have highlighted the importance of the II–III cytoplasmic loop of the α1 subunit of the DHPr in these interactions (1–3). Within this loop, a 20 amino acid fragment named domain A has received particular attention because the corresponding isolated peptide is capable of modulating Ca^{2+} release from SR preparations as well as the activity of the isolated RYr channel (4–9). The situation is, however, not absolutely clear because both activating and inhibiting effects have been reported. Furthermore, the relevance and exact function of this segment during physiological e-c coupling have been seriously challenged by negative results in studies that used expression of chimeras of the α1 subunit in dysgenic myotubes (10–12).

MCa is a 33 amino acid toxin isolated from the venom of the scorpion *Scorpio maurus palmatus* (13). MCa is very similar to Imperatoxin A (IpTxa), a venom toxin from another scorpion, and both share some sequence homology and a striking similarity in the spatial orientation of positively charged residues with domain A of the II–III loop of the DHPr (see 14,15). Interestingly both MCa and IpTxa can enhance [^{3}H]ryanodine binding to SR vesicles, increase ion flow through isolated ryanodine receptors, elicit Ca^{2+} release from SR vesicles, and modulate the properties of elementary calcium release events detected in permeabilized muscle fibers (6,13,14,16–19). In the case of MCa, there is also clear evidence that it binds to the same site of the RYr as domain A (20). This potentially makes these two toxins highly interesting tools to characterize the still elusive role of domain A of the DHPr in the e-c coupling process. Here we injected MCa into adult skeletal muscle fibers from mouse and measured intracellular [Ca^{2+}] under voltage-clamp conditions. Results show that MCa dramatically affects the process of repolarization-induced closure of the RYrs during physiological e-c coupling.

Submitted November 18, 2005, and accepted for publication June 7, 2006.

Address reprint requests to Vincent Jacquemond, Physiologie Intégrative Cellulaire et Moléculaire, Université Claude Bernard Lyon 1, UMR CNRS 5123, Bât. Raphael Dubois, 43 boulevard du 11 novembre 1918, F 69622 Villeurbanne Cedex, France. Tel.: 33-4-72-44-81-64; Fax: 33-4-72-44-79-37; E-mail: vincent.jacquemond@univ-lyon1.fr.

0006-3495/06/09/2206/10 $2.00

doi: 10.1529/biophysj.105.078089

METHODS

Preparation of the muscle fibers

Experiments were performed on single fibers isolated from the flexor digitorum brevis (fdb) muscles from 4- to 8-week-old Swiss OF1 mice. All experiments were performed in accordance with the guidelines of the French Ministry of Agriculture (87/848) and of the European Community (86/609/EEC). Procedures for enzymatic isolation of single muscle fibers, partial insulation of the fibers with silicone grease, and intracellular microinjection of the dye indo-1 were as described previously (21–24). In brief, the major part of a single fiber was electrically insulated with silicone grease so that whole-cell voltage clamp could be achieved on a short portion of the fiber extremity. Before the voltage-clamp, indo-1 was introduced into the myoplasm through local pressure microinjection. Intracellular loading of either MCa or its mutated analog [Ala^{24}]MCa was achieved by coinjection with the dye; peptides were present in the microinjected solution at a concentration of 100 μM. Following diffusion and equilibration within the cytoplasm, this was believed to achieve a final cytoplasmic concentration within the 10 μM range (for details concerning microinjections, see Csernoch et al. (25)). It should be noted that the effects seen in the present study required two orders of magnitude more MCa than experiments in more isolated systems. One likely reason for this discrepancy is that most of the injected MCa was bound to sites within the fiber so that the free MCa concentration was very much lower than the above estimated level.

In a separate series of experiments, we also tested the effect of the injection of a synthetic domain A peptide corresponding to residues Thr^{671}–Leu^{690} of the α1 subunit of the DHPr; this peptide was used at a concentration of 2 mM in the injecting pipette.

Control data were always obtained from fibers issued from the same muscles as the toxin- or peptide-injected fibers. The number of fibers tested under a given set of conditions was always obtained from muscles taken from at least three different animals.

All experiments were performed at room temperature (20–22°C).

Electrophysiology

An RK-400 patch-clamp amplifier (Bio-Logic, Claix, France) was used in whole-cell configuration. Command voltage pulse generation and data acquisition were done using commercial software (Biopatch Acquire, Bio-Logic) driving an A/D, D/A converter (Lab Master DMA board, Scientific Solutions, Mentor, OH). Analog compensation was systematically used to decrease the effective series resistance. Voltage clamp was performed with a microelectrode filled with the intracellular-like solution (see Solutions). The tip of the microelectrode was inserted through the silicone, within the insulated part of the fiber. Membrane depolarizations (or series of depolarizations) were applied every 30 s from a holding command potential of −80 mV.

Fluorescence measurements

The optical set-up and the procedures used for indo-1 fluorescence measurements were as described previously (21–23,26). In brief, a Nikon Diaphot epifluorescence microscope was used in diafluorescence mode. The beam of light from a high-pressure mercury bulb set on the top of the microscope was passed through a 335-nm interference filter and focused onto the preparation. The emitted indo-1 fluorescence light was collected by a ×40 objective and simultaneously detected at 405 ± 5 nm (F_{405}) and 470 ± 5 nm (F_{470}) by two photomultipliers. The fluorescence measurement field was 40 μm in diameter, and the silicone-free extremity of each tested fiber was placed in the middle of the field. Background fluorescence at both emission wavelengths was measured next to each tested fiber and was then subtracted from all measurements.

Calibration of the indo-1 response and [Ca^{2+}]$_i$ calculation

The standard ratio method was used with the parameters $R = F_{405}/F_{470}$ and R_{min}, R_{max}, K_D, and β having their usual definitions. Results were either expressed in terms of indo-1 percentage saturation or in actual free calcium concentration (for details of calculation, see Jacquemond (21) and Csernoch et al. (25)). In vivo values for R_{min}, R_{max}, and β were measured using procedures described previously (22,23).

Calculation of the rate of calcium release

The method used to estimate the SR calcium release flux from the indo-1 transients was previously described (24): the time derivative of the total myoplasmic Ca^{2+} was calculated from the occupancy of the main intracellular calcium binding sites (27). The model included troponin C binding sites with a total sites concentration TN_{total} of 250 μM, an ''on'' rate constant $k_{on,CaTN}$ of 0.0575 $\mu M^{-1}\cdot ms^{-1}$ and an ''off'' rate constant $k_{off,CaTN}$ of 0.115 ms^{-1}; Ca-Mg binding sites on parvalbumin with a total sites concentration PV_{total} = 700 μM, ''on'' rate constant for Ca^{2+} $k_{on,CaPV}$ = 0.125 $\mu M^{-1}\cdot ms^{-1}$, ''off'' rate constant for Ca^{2+} $k_{off,\ CaPV} = 5 \times 10^{-4}$ ms^{-1}, ''on'' rate constant for Mg^{2+} $k_{on,\ MgPV} = 3.3 \times 10^{-5}$ $\mu M^{-1}\cdot ms^{-1}$, ''off'' rate constant for Mg^{2+} $k_{off,\ MgPV} = 3 \times 10^{-3}$ ms^{-1}. The rate of calcium transport across the SR membrane was assumed to be proportional to the fractional occupancy of the SR pump sites with a dissociation constant $K_{d\ Capump}$ of 2 μM and a maximum pump rate of 3 $\mu M\cdot ms^{-1}$. Resting [Mg^{2+}] was assumed to be 1.5 mM. Indo-1 was assumed to be present at 100 μM with values for the ''on'' and ''off'' rate constants of the Ca-indo-1 binding reaction of 1×10^8 $M^{-1}\cdot s^{-1}$ and 30 s^{-1}, respectively.

Simulation of indo-1 transients

Simulations of [Ca-indo-1] transients elicited by membrane depolarizations were performed according to the procedure of Timmer et al. (28), as described in Collet et al. (23). In brief, a synthetic Ca^{2+} release rate waveform was fed into a calcium distribution model that reproduced the main features of Ca^{2+} regulation in a muscle fiber. The model included the intracellular Ca^{2+} binding sites and uptake mechanism described in the previous paragraph. Resting [Ca^{2+}] was assumed to be 0.1 μM.

Solutions

The intracellular-like solution contained (in mM) 120 K-glutamate, 5 Na_2-ATP, 5 Na_2-phosphocreatine, 5.5 $MgCl_2$, 5 glucose, and 5 HEPES adjusted to pH 7.20 with KOH. The standard extracellular solution contained (in mM) 140 TEA-methanesulfonate, 2.5 $CaCl_2$, 2 $MgCl_2$, 10 TEA-HEPES, and 0.002 tetrodotoxin, pH 7.20.

Statistics

Least-squares fits were performed using a Marquardt-Levenberg algorithm routine included in Microcal Origin (Originlab, Northampton, MA). Data values are presented as means ± SE for n fibers, where n is specified in Results. Statistical significance was determined using a Student's t-test assuming significance for $p < 0.05$.

RESULTS

The effects of MCa and of its mutated inactive analog [Ala^{24}]MCa (14) were tested on membrane current and intracellular calcium measured from isolated mouse skeletal muscle fibers. The mean initial resting [Ca^{2+}] level did not differ significantly among control fibers (58 ± 12 nM,

$n = 16$), MCa-injected fibers (49 ± 6 nM, $n = 22$), and [Ala^{24}]MCa-injected fibers (62 ± 11 nM, $n = 7$), indicating that the peptides did not chronically alter the intracellular resting Ca^{2+} homeostasis. However, the presence of MCa produced a very remarkable change in the properties of the voltage-activated Ca^{2+} transients. This is illustrated in Fig. 1 *A*, which shows superimposed indo-1 calcium signals that were elicited by successive step membrane depolarizations of 10, 30, and 50 ms duration to +10 mV in a control fiber, an MCa-injected fiber, and an [Ala^{24}]MCa-injected fiber. In all fibers, and as classically described, voltage-activated SR Ca^{2+} release produced a rapid rise in the calcium indicator saturation level, and the signal remained elevated during the pulse. In the control fiber and in the [Ala^{24}]MCa-injected fiber, membrane repolarization turned off Ca^{2+} release, and as a consequence, the indo-1 signal returned toward its resting level with a time constant in the hundreds of milliseconds range, as typically observed under normal conditions (see, for example, Jacquemond (21), Collet et al. (22), and Pouvreau et al. (26)). In the MCa-injected fiber, there was also a repolarization-induced sharp decay of the indo-1 signal, but surprisingly, the decline was only partial, and the signal was still very much elevated at the end of the records. Pulses of 10 and 30 ms duration to +10 mV were applied in several fibers issued from the same muscles under these three conditions. The graphs in Fig. 1 give mean values for the corresponding baseline $[Ca^{2+}]$ level (Fig. 1 *B*), the peak $\Delta[Ca^{2+}]$ during the pulse (Fig. 1 *C*), the $\Delta[Ca^{2+}]$ measured at the time of the end of the records shown in Fig. 1 *A* (Fig. 1 *D*, which is 0.92 s after the onset of the pulses, which we will refer to as 1 s after the pulses for simplicity), and the ratio of $\Delta[Ca^{2+}]$ measured 1 s after the pulse ($\Delta[Ca^{2+}]_{1s}$) to the preceding peak $\Delta[Ca^{2+}]$ (Fig. 1 *E*). Ca^{2+} values were obtained without correction for the kinetics of indo-1 Ca-binding. Fibers were all challenged successively with 10- and 30-ms-long pulses, with records taken either as shown in Fig. 1 *A* or with longer records taken at a slower sampling rate (as shown in Fig. 2). There was no significant difference in the baseline $[Ca^{2+}]$ (Fig. 1 *B*) and peak $\Delta[Ca^{2+}]$ level (Fig. 1 *C*) among the three groups of fibers. Conversely, the mean absolute $\Delta[Ca^{2+}]$ measured 1 s after the pulse was significantly larger, for both pulse durations, in the MCa-injected fibers than in either the control fibers or the [Ala^{24}]MCa-injected fibers (Fig. 1 *D*). On average the $\Delta[Ca^{2+}]_{1s}$ value was ~30% of the preceding peak $\Delta[Ca^{2+}]$ in the MCa-injected fibers and ~5% in the control and in the [Ala^{24}]MCa-injected fibers (Fig. 1 *E*). The fact that this ratio exhibited a similar value for the two pulse durations in the presence of MCa indicates that the amplitude of the phenomenon correlated well with the preceding extent of Ca^{2+} release activation during the pulse.

In Fig. 1 *A*, it is noticeable that within the 30-s period of time between two consecutive pulses, $[Ca^{2+}]$ had eventually returned to its initial resting level as witnessed by the absence of change in the baseline indo-1 saturation level. The MCa-induced sustained postpulse $[Ca^{2+}]$ level was thus a transient phenomenon. Examples of its overall time course are illustrated in Fig. 2, which shows 15-s-long indo-1 saturation records in a control fiber and in two MCa-injected fibers. Fibers were depolarized by short pulses to +10 mV of various durations. Although somewhat variable in pattern and amplitude, the postpulse $[Ca^{2+}]$ elevation observed in the presence of MCa always lasted for seconds and vanished with an extremely slow time course.

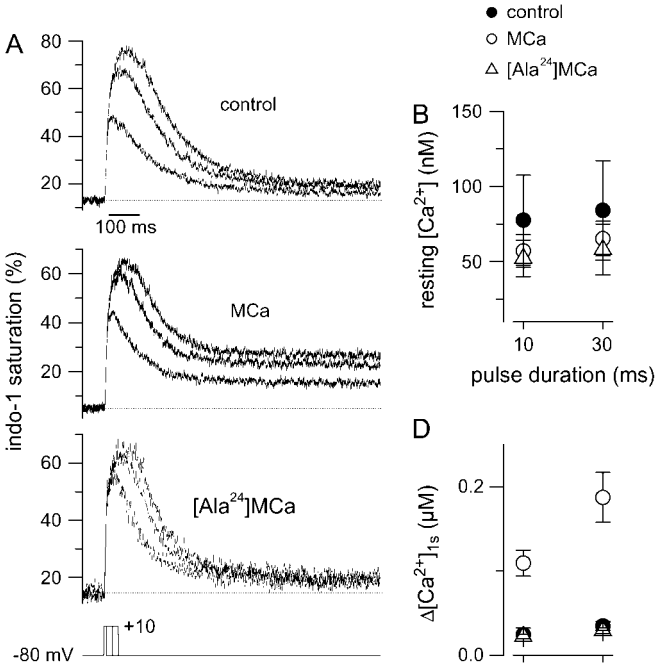

FIGURE 1 Incomplete decay of step depolarization-activated Ca^{2+} transients in MCa-injected fibers. (*A*) Indo-1 saturation transients elicited by consecutive depolarizing steps of 10, 30, and 50 ms duration to +10 mV in a control fiber (*top*) in an MCa-injected fiber (*middle*), and in a fiber injected with the mutated analog [Ala^{24}]MCa. (*B*) Mean values for the baseline $[Ca^{2+}]$ level in control ($n = 5$), MCa-injected ($n = 9$), and [Ala^{24}]MCa-injected fibers ($n = 5$) challenged by a 10- and a 30-ms-long pulse to +10 mV. (*C* and *D*) Corresponding values for the peak $\Delta[Ca^{2+}]$ and the $\Delta[Ca^{2+}]$ measured ~1 s after the onset of the pulse, respectively. (*E*) Corresponding mean values for the ratio of the $\Delta[Ca^{2+}]$ measured ~1 s after the onset of the pulse (mean shown in *C*) to the peak $\Delta[Ca^{2+}]$ during the pulse (mean shown in *D*). See text for details.

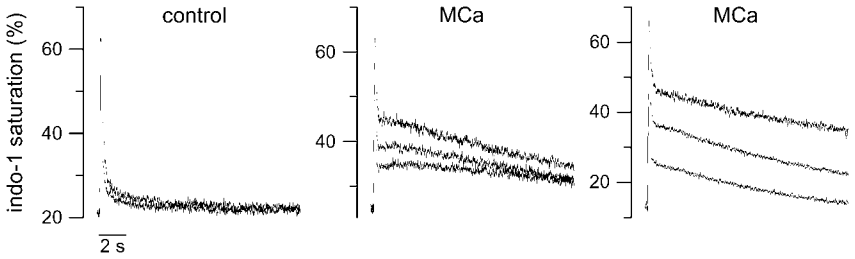

FIGURE 2 The long-lasting [Ca^{2+}] elevation following the end of a step depolarization in MCa-injected fibers. Traces correspond to indo-1 saturation records of 15 s duration in a control fiber and in two MCa-injected fibers depolarized by short pulses to +10 mV of various durations. Pulses of 5 and 10 ms duration were applied in the control fiber (*left*). Pulses of 5, 10, and 30 ms duration were applied in the two MCa-injected fibers.

This long-lasting elevated intracellular [Ca^{2+}] level had to result from either an additional influx of Ca^{2+} into or a reduced Ca^{2+} efflux from the myoplasm. The possibility that MCa produced an extra Ca^{2+} influx across the plasma membrane following a step membrane depolarization is unlikely because there was no specific change in the membrane current during and after the pulses in the MCa-injected fibers, as compared to the control ones. This is illustrated in Fig. 3, which shows indo-1 calcium transients and corresponding membrane current traces displayed at a high *y*-scale magnification, elicited by three consecutive 5-ms-long pulses to +10 mV applied to a control fiber (Fig. 3 *A*) and to an MCa-injected fiber (Fig. 3 *B*). Although the presence of MCa induced a very reproducible long-lasting Ca^{2+} elevation after each of the pulses, the membrane current traces were very similar to those from the control fiber. From data from the fibers used in Fig. 1, the mean change in membrane current ΔI (from the prepulse holding level) measured at the end of the 10-ms-long pulses was -0.21 ± 0.3 ($n = 3$), 0.72 ± 0.41 ($n = 5$), and 1.46 ± 0.8 ($n = 5$) A/F in control fibers, MCa-injected fibers, and [Ala^{24}]MCa-injected fibers, respectively. When measured 1 s after the pulse, ΔI was -0.024 ± 0.006 ($n = 5$), -0.021 ± 0.004 ($n = 9$), and -0.01 ± 0.004 A/F ($n = 5$) in the same groups, respectively. For the two sets of measurements there was no significant difference among the three groups.

Furthermore, in three fibers injected with MCa, we took measurements in the presence and in the absence of extracellular calcium. For this, each tested cell was superfused continuously with the extracellular solution using a polyethylene capillary perfusion system operated by gravity. Fig. 4 shows membrane currents and indo-1 calcium signals measured from one of these fibers in response to a 20-ms-long voltage step to +10 mV in the control condition (left), in the absence of extracellular calcium (replaced by magnesium, middle), and after returning to the control calcium-containing solution (wash, right). The membrane current records are presented on an expanded *x* scale for clarity. They were corrected for the passive linear components by subtracting the adequately scaled current measured in response to a 20-mV hyperpolarization. The membrane current traces in the presence of the control external solution clearly exhibit a negative inward phase because of the activation of the slow inward calcium current (see, for instance, Collet et al. (30)). As expected, this current was lost in the absence of extracellular calcium, but there was no simultaneous effect on the amplitude of the postpulse sustained phase of [Ca^{2+}] elevation that resulted from the presence of MCa. In

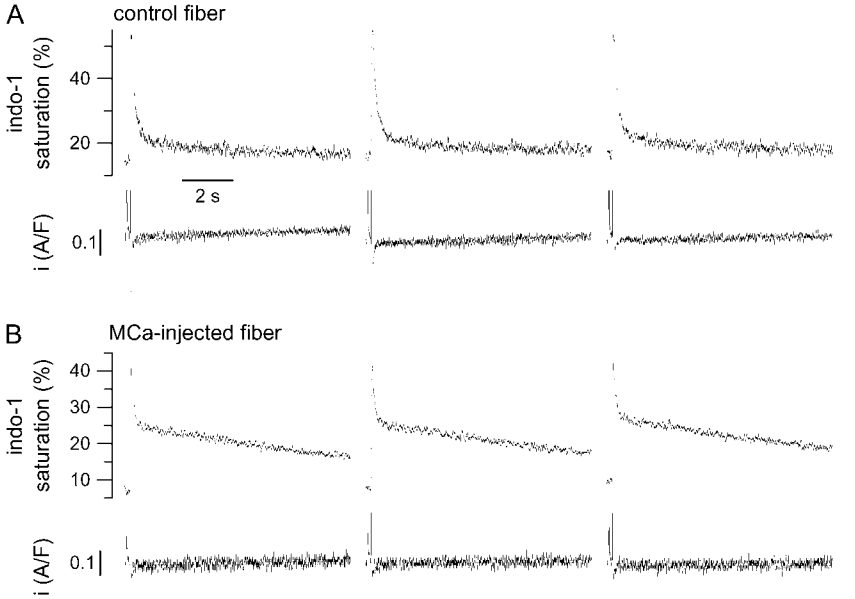

FIGURE 3 The MCa-induced long-lasting postpulse [Ca^{2+}] elevation is not associated with a change in the holding membrane current. In *A* and *B*, the top series of traces correspond to successive (*from left to right*) indo-1 saturation transients elicited by a 5-ms-long pulse to +10 mV in a control fiber (*A*) and in an MCa-injected fiber (*B*); the bottom series of traces show the corresponding membrane current records at a high gain.

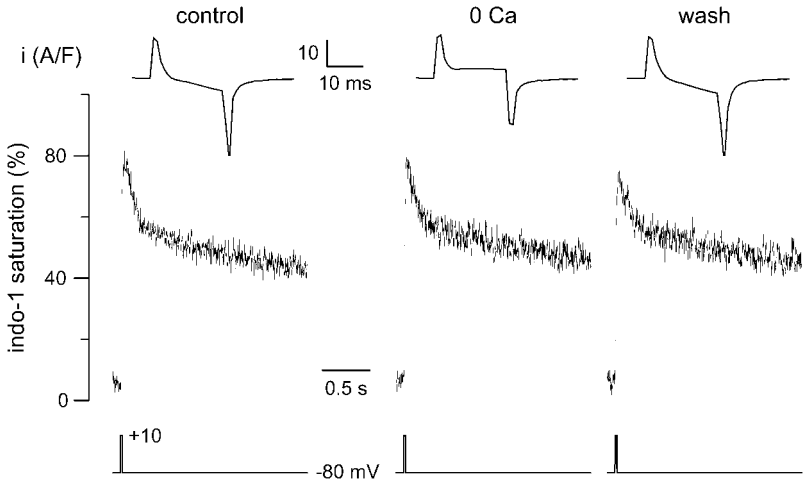

FIGURE 4 The MCa-induced long-lasting postpulse [Ca^{2+}] elevation persists in the absence of extracellular calcium. All records are from the same fiber injected with MCa. The top series of traces corresponds to the changes in membrane current elicited by a 20-ms-long pulse to +10 mV. The indo-1 calcium signals measured simultaneously are shown underneath on a more compressed timescale. Records were taken in the presence of the control extracellular solution (*left*), in the absence of extracellular calcium (*middle*), and after returning to the calcium-containing control solution (*right*). Membrane current records were corrected for the linear components.

the three fibers tested, the peak change in Ca^{2+} measured 1 s after the end of the pulse in the absence of extracellular calcium corresponded to 86 ± 9% of the value measured previously in the presence of extracellular calcium. We believe that this definitely excludes the possibility of a significant contribution of external calcium to the effect of MCa.

The MCa-induced postpulse elevated Ca^{2+} level was thus of intracellular origin. Because the phenomenon was triggered only upon voltage activation of the fibers, and because the initial fast decline of the calcium transients appeared unaffected, there is little doubt that the underlying mechanism was a transient dysfunction of SR Ca^{2+} release. This, of course, is also in agreement with the results from previous measurements on SR vesicles and single ryanodine receptor channels that showed a selective effect of MCa on the calcium release channel activity with no concurrent alteration of the SERCA-mediated Ca^{2+} uptake (14,29). The features of the MCa-induced postpulse Ca^{2+} elevation are consistent with a slowly decaying extra phase of Ca^{2+} release proceeding for seconds following membrane repolarization. This is simulated in Fig. 5 using a model of calcium distribution (see Methods). Fig. 5 *A* shows synthetic Ca^{2+} release flux traces in control conditions (thin trace) and in the presence of MCa (thick trace). The inset in Fig. 5 *A* shows an enlarged view of the Ca^{2+} release flux traces assumed to be activated by the depolarizing voltage step (V). The Ca^{2+} flux waveform was made to have an early transient component that spontaneously decayed during the pulse toward a steady level. Upon repolarization, the flux was made to turn off with a time constant of 3 ms. Fig. 5 *B* shows the same traces on a longer timescale. The control and the MCa flux traces were made to be identical until the end of the pulse; thereafter, the difference between the two was the presence of an additional small slowly decaying extra phase of Ca^{2+} release in the MCa trace. This slowly decaying component was simulated as having a single exponential time course with a time constant of 8 s and an amplitude of 0.2 μM/ms. Fig. 5, *C* and *D*, show the indo-1 saturation traces calculated from the above fluxes on a short and a long timescale, respectively. Results clearly show that a slowly decaying postpulse extra Ca^{2+} flux can well account for the results obtained in the presence of MCa.

We also took advantage of the simulation to quantitatively estimate the amplitude of the transmembrane calcium current that would have been necessary to account for the observed

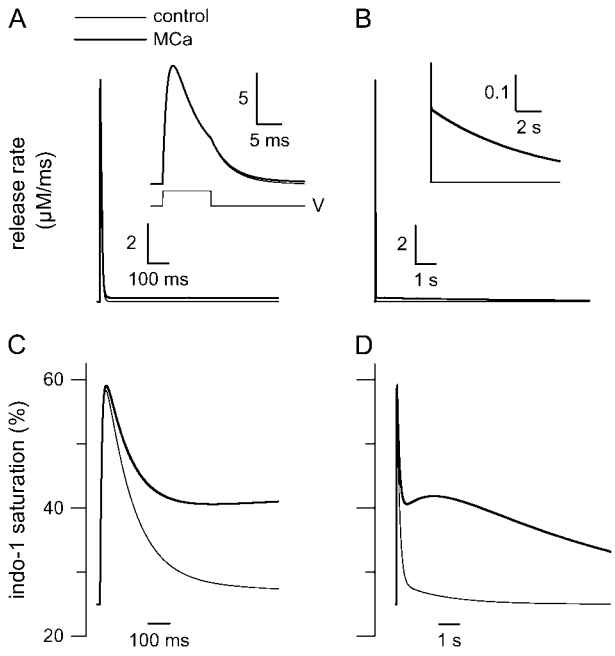

FIGURE 5 Simulation of the effect of MCa using a simple model of intracellular Ca^{2+} distribution. (*A* and *B*) Synthetic Ca^{2+} release flux traces in control conditions (*thin trace*) and in the presence of MCa (*thick trace*). In *A* and *B* the same traces are shown on a short and long timescale, respectively. In *A*, the inset focuses on the peak phase of the release traces. In *B*, the inset shows the two traces on an expanded *y* scale. The only difference between the control and the MCa trace is the presence of a small slowly decaying extra phase of Ca^{2+} release in the presence of MCa. This extra phase is best seen in the inset of panel *B*. (*C* and *D*) Corresponding calculated indo-1 saturation traces on short and long timescales, respectively.

effect of MCa (if the effect were to be solely through Ca^{2+} entry across the plasma membrane). Using a value of 40 μm for the diameter of the voltage-clamped end portion of the fiber and assuming a ratio of capacitance to apparent membrane surface of 5 $\mu F/cm^2$ (21,30) and a fraction of total fiber volume accessible to Ca^{2+} of 0.7, the MCa-induced extra Ca^{2+} input flux of 0.2 μM/ms peak amplitude in Fig. 5 would have corresponded to a peak transmembrane calcium current of ~5 A/F amplitude. Because such a current was clearly absent from the records obtained in the presence of MCa (Fig. 3), this possibility was definitely discarded, in accordance with the results from Fig. 4.

As already pointed out in Fig. 1 and also observable in Fig. 2, a specific feature of the MCa effect was that the amplitude of the postpulse $[Ca^{2+}]$ elevation was larger as the pulse duration was increased, indicating that the size of the postpulse uncontrolled Ca^{2+} flux depended on the previous extent of voltage-dependent Ca^{2+} release activation. This

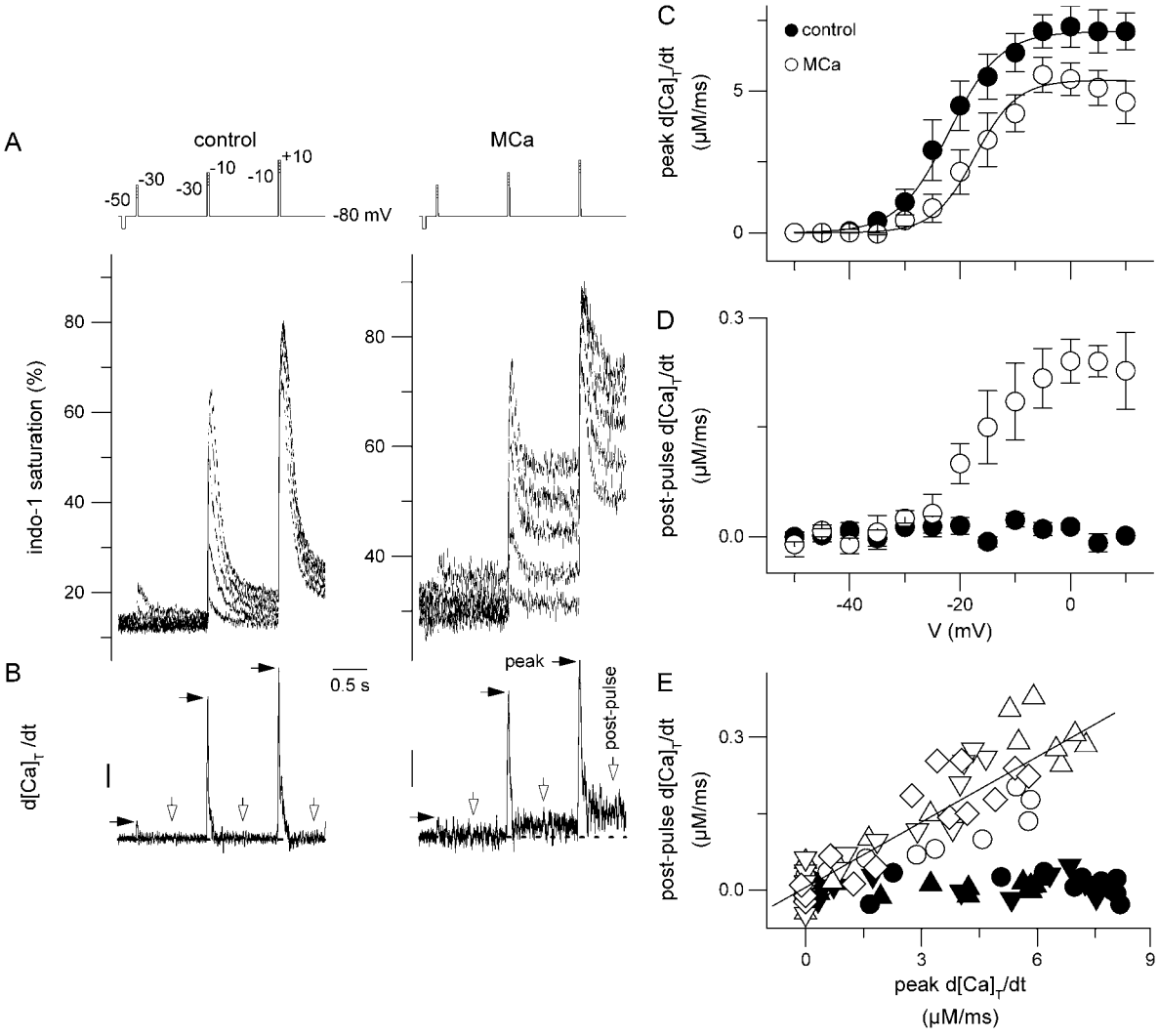

FIGURE 6 Voltage dependence of Ca^{2+} release in control fibers and in MCa-injected fibers. (*A*) Indo-1 saturation transients measured in response to the pulse protocol illustrated on top, in a control fiber (*left*) and in an MCa-injected fiber (*right*). The protocol consisted of a sequence of three consecutive step depolarizations of 30 ms duration. During the first sequence the three successive steps were to −50, −30, and −10 mV, respectively. The amplitude of each of the three steps was then incremented by 5 mV, and the sequence was repeated. The sequence was applied five times so that during the last run the three steps were to −30, −10, and +10 mV, respectively. Indo-1 transients obtained in response to the five sequences are shown superimposed. (*B*) Ca^{2+} release flux calculated from the above indo-1 transients; only the release flux from the indo-1 trace obtained in response to the successive pulses to −30, −10, and +10 mV is shown. The *y* scale bar in each panel corresponds to 1 μM/ms. The horizontal dotted line corresponds to the initial baseline level. Solid and open arrows point to the peak and postpulse release flux levels that were measured, respectively; amplitudes were measured from the prepulse level. The postpulse flux values were taken as the average from a 100-ms-long portion of trace 500 ms following the pulse onset. The mean from these measurements is reported in the following panels. (*C*) Mean voltage dependence of the peak Ca^{2+} release flux in control fibers (*solid circles, n* = 3) and in MCa-injected fibers (*open circles, n* = 4). (*D*) Corresponding mean voltage dependence of the postpulse Ca^{2+} release flux. (*E*) Plot of the individual values of the postpulse release flux versus the corresponding peak release flux in the control (*solid symbols*) and the MCa-injected fibers (*open symbols*). Different symbols correspond to the different fibers.

was also true when, for the same duration, the pulse amplitude was increased within the voltage range of activation of Ca^{2+} release (see Fig. 6 *A*). This suggests that the more release channels are activated by voltage, the more will potentially be affected by MCa and remain open after membrane repolarization. Despite its impressive effect on the postpulse [Ca^{2+}] level, MCa seemed to only marginally, if at all, affect Ca^{2+} release during the depolarizing pulses. As an example, Fig. 6 shows the results from experiments aimed at comparing the voltage dependence of Ca^{2+} release between control and MCa-injected fibers. Indo-1 Ca^{2+} signals were recorded in response to the pulse protocol shown at the top of Fig. 6 *A*. It consisted of a sequence of three consecutive step depolarizations of 30 ms duration to the indicated values; each pulse was then incremented by 5 mV, and the sequence was repeated. Fig. 6 *A* shows an example of corresponding indo-1 saturation signals in a control fiber and in an MCa-injected fiber, whereas Fig. 6 *B* shows the Ca^{2+} release traces ($d[Ca]_T/dt$, see Methods) calculated from the above transients. For clarity only the release flux trace calculated from the last sequence of indo-1 transients (in response to the pulses to −30, −10, and +10 mV) is shown. Although during a single sequence the sustained postpulse [Ca^{2+}] level in the presence of MCa may have affected the properties of Ca^{2+} release during the next pulse, the voltage levels for both threshold and maximal activation of Ca^{2+} release were similar in the two fibers. The mean voltage dependence of the peak Ca^{2+} release flux from identical experiments in three control fibers and four MCa-injected fibers is shown in Fig. 6 *C*. Superimposed curves were calculated with the mean parameters obtained from fitting a Boltzmann function to the individual series of data points in each fiber. Mean corresponding values for the peak release flux, midpoint voltage, and steepness factor were 7.1 ± 0.6 μM/ms, −22 ± 2 mV, and 4.6 ± 0.3 mV in control fibers and 5.4 ± 0.5 μM/ms, −17.3 ± 3 mV, 3.8 ± 0.1 mV in MCa-injected fibers, respectively. Mean values for the peak release flux and midpoint voltage did not significantly differ, whereas the steepness factor was slightly but significantly reduced in the presence of MCa ($p = 0.05$). Fig. 6 *D* presents the voltage dependence of the mean values for the postpulse release flux in the control and in the MCa-injected fibers; values were measured 500 ms following the onset of each pulse (time indicated by the open arrows in panel *B*). In the MCa-injected fibers, the amplitude of the postpulse flux clearly had a voltage dependence similar to that of the peak release flux, whereas the control fibers exhibited no residual postpulse flux. The strong dependence of the amplitude of the postpulse release flux on the amplitude of the peak flux is further illustrated in Fig. 6 *E*, where corresponding individual values for these two parameters were plotted versus each other. Fitting a straight line through the individual series of MCa data points in each fiber indicated that the postpulse release flux corresponded to 4.3 ± 0.005% of the peak flux activated during the pulse.

Because MCa presents some homology with domain A of the II–III loop of the α1 subunit of the DHPr, it was of particular interest to directly test the effect of domain A under the present conditions. A series of measurements was thus performed with fibers microinjected with a synthetic domain A peptide (see Methods). Fig. 7 illustrates a series of results from these experiments; this figure is organized in the same format as Fig. 1 to ease the comparison. Fig. 7 *A* shows superimposed indo-1 calcium signals elicited by step depolarizations of 10, 20, and 50 ms duration to +10 mV in a control fiber and in a fiber injected with the domain A peptide. The graphs give mean values for the corresponding baseline [Ca^{2+}] level (Fig. 7 *B*), the peak Δ[Ca^{2+}] during the

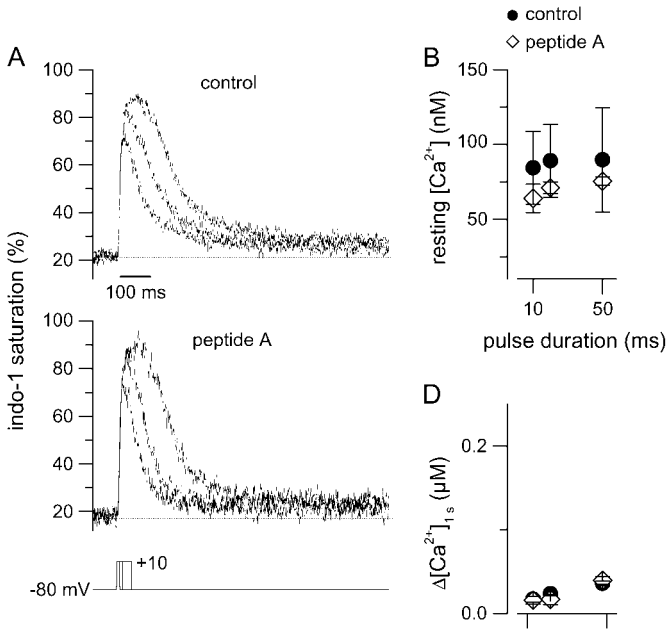

FIGURE 7 Voltage-activated Ca^{2+} transients in fibers injected with a synthetic peptide corresponding to domain A of the II–III loop of the DHPr α1 subunit. (*A*) Indo-1 saturation transients elicited by consecutive depolarizing steps of 10, 20, and 50 ms duration to +10 mV in a control fiber (*top*) and in a peptide A-injected fiber (*bottom*). (*B*) Mean values for the baseline [Ca^{2+}] level in control ($n = 4$) and peptide A-injected fibers ($n = 4$) challenged by the pulse protocol shown in *A*. (*C* and *D*) Corresponding values for the peak Δ[Ca^{2+}] and the Δ[Ca^{2+}] measured ~1 s after the onset of the pulse, respectively. (*E*) Corresponding mean values for the ratio of the Δ[Ca^{2+}] measured ~1 s after the onset of the pulse (mean shown in *C*) to the peak Δ[Ca^{2+}] during the pulse (mean shown in *D*).

pulse (Fig. 7 *C*), the $\Delta[Ca^{2+}]$ measured 0.92 s (referred to as 1 s) after the onset of the pulses (Fig. 7 *D*), and the ratio of $\Delta[Ca^{2+}]$ measured 1 s after the pulse ($\Delta[Ca^{2+}]_{1s}$) to the preceding peak $\Delta[Ca^{2+}]$ (Fig. 7 *E*). The *y* scale in panels *B*, *D*, and *E* is the same as in the corresponding panels of Fig. 1. Data are from four control fibers and four fibers injected with peptide A. Obviously, the presence of peptide A in the intracellular medium did not produce any reproducible alteration in the properties of the Ca^{2+} transients that would be consistent with the effect of MCa.

DISCUSSION

The present results show that during physiological excitation–contraction coupling, the step of repolarization-induced closure of the Ca^{2+} release channels is transiently disrupted by MCa, a toxin peptide that exhibits some homology with domain A of the II–III loop of the DHPr in terms of both amino acid sequence (13) and three-dimensional structure (31). MCa was previously shown to have potentiating or activating effects on [^{3}H]ryanodine binding to and Ca^{2+} release from SR vesicles, on isolated RYr channel activity, on Ca^{2+} release from intact myotubes, and on spontaneous Ca^{2+} release events in permeabilized muscle fibers (13,14,19,29). More recently MCa and domain A were shown to share common binding sites on RYr1 (20), which, added to the fact that MCa effect on RYr1 is clearly inhibited by domain A (29), would provide convincing support for the possibility that the two act on the same target through an analogous mechanism. The fact that the inhibition did not correspond to a simple competitive process (29) is likely to be related to the complexity of the overall mechanism because of the presumable 4:1 stoichiometry of the MCa (or domain A)-RYr1 interaction.

Here we show that, within the physiological operating mode of e-c coupling of an intact mammalian skeletal muscle fiber, MCa forces Ca^{2+} release channels to remain open following a transient membrane depolarization. The effect of MCa was specific because a single amino-acid substitution (Arg^{24} by an alanine), previously shown to prevent MCa alteration of RYr1 activity (14), induced the loss of its effectiveness. The simplest conclusion from our results is that repolarization-induced closure of MCa-modified RYr channels is temporarily impaired. At this point two alternatives may be considered.

The first possibility would be that the effects of MCa arise from its homology with domain A and tell us something about the dynamic physiological interactions that take place between the DHPr and the RYr during e-c coupling. In this framework however, one may have expected an excess of free peptide A in the myoplasm to produce a similar effect to that of MCa. In contrast, fibers injected with a synthetic domain A peptide did not exhibit a sustained Ca^{2+} elevation following a step depolarization. This makes it hard to argue further in favor of this first hypothesis, although it remains possible that the synthetic domain A peptide does not yield the exact native functional configuration of the corresponding endogenous segment within the II–III loop or that the exogenous domain A is functional but acts in an undistinguishable manner from the endogenous one. Alternatively, the difference observed here between peptide A and MCa in terms of functional effect may be related to the biochemical and single-channel data indicating that peptide A does not compete with MCa (29) or IpTx A (32) for certain effects on the ryanodine receptor. Finally, although here we did not detect any obvious effect of peptide A, it should be mentioned that in mechanically skinned rat skeletal muscle fibers with functional excitation-contraction coupling, peptide A was reported to elicit small spontaneous force responses in some fibers and to potentiate responses to depolarization in all fibers (33).

Despite the sequence homology between domain A of the DHPr and MCa and their common binding site on the RYr, it is also possible that MCa acts through a mechanism that is independent of the function of domain A. Because the toxin had no detectable effect on resting $[Ca^{2+}]$ in the absence of depolarization, MCa is likely to have poor access to its binding site under resting conditions. Depolarization-induced opening of the RYr channels most likely then reveals the MCa binding site, allowing interaction with the toxin. Ca^{2+} transients exhibited no major alteration during the depolarizing pulses in the presence of MCa: the absolute peak amplitude of the transients and the voltage dependence of Ca^{2+} release were similar to those observed under control conditions. MCa thus does not appear to strongly impair the functional operating mode of the overall population of RYr channels once the membrane is depolarized. This may indicate that MCa-bound channels behave normally during the depolarization, though one also cannot exclude the possibility that the fraction of MCa-bound channels was low enough that even if operating in an altered mode their contribution would be too little to seriously affect the overall release flux during the pulse. Conversely, membrane repolarization clearly reveals the activity of the MCa-bound channels. Once bound, MCa thus likely prevents the conformational change required for channel closure upon membrane repolarization. In that sense, MCa could be pictured to act in an analogous way as ryanodine, which, as we have previously showed, produces a use-dependent increase in SR Ca^{2+} leak because RYr channels remain locked open after a transient membrane depolarization (23). A noticeable difference is, however, that MCa-modified channels eventually return to a normal gating mode, presumably as a result of the dissociation of MCa, as indicated by the return of intracellular $[Ca^{2+}]$ to its resting level.

The present effect of MCa has a striking similarity with a previously described alteration of e-c coupling in frog skeletal muscle, where low myoplasmic $[Mg^{2+}]$ levels could also induce a long-lasting elevation of myoplasmic $[Ca^{2+}]$ following a transient membrane depolarization (34). The

similarity with the present effect of MCa may indicate that the putative site for Mg^{2+} inhibition of Ca^{2+} release is somehow linked to the MCa binding site.

In conclusion, this work demonstrates that the scorpion venom toxin MCa specifically alters the physiological process of repolarization-induced closure of the RYr channels. Further investigation of the properties of this effect will certainly prove helpful to unravel the molecular steps involved in the control of the RYr channels during excitation-contraction coupling.

This work was supported by grants from Centre National de la Recherche Scientifique (CNRS), University Claude Bernard Lyon 1, and Association Française contre les Myopathies.

REFERENCES

1. Tanabe, T., K. G. Beam, B. A. Adams, T. Niidome, and S. Numa. 1990. Regions of the skeletal muscle dihydropyridine receptor critical for excitation-contraction coupling. *Nature*. 346:567–569.
2. Lu, X., L. Xu, and G. Meissner. 1994. Activation of the skeletal muscle calcium release channel by a cytoplasmic loop of the dihydropyridine receptor. *J. Biol. Chem.* 269:6511–6516.
3. Nakai, J., T. Tanabe, T. Konno, B. Adams, and K. G. Beam. 1998. Localization in the II–III loop of the dihydropyridine receptor of a sequence critical for excitation-contraction coupling. *J. Biol. Chem.* 273:24983–24986.
4. El-Hayek, R., B. Antoniu, J. Wang, S. L. Hamilton, and N. Ikemoto. 1995. Identification of calcium release-triggering and blocking regions of the II–III loop of the skeletal muscle dihydropyridine receptor. *J. Biol. Chem.* 270:22116–22118.
5. Dulhunty, A. F., D. R. Laver, E. M. Gallant, M. G. Casarotto, S. M. Pace, and S. Curtis. 1999. Activation and inhibition of skeletal RyR channels by a part of the skeletal DHPR II–III loop: effects of DHPR Ser687 and FKBP12. *Biophys. J.* 77:189–203.
6. Gurrola, G. B., C. Arevalo, R. Sreekumar, A. J. Lokuta, J. W. Walker, and H. H. Valdivia. 1999. Activation of ryanodine receptors by imperatoxin A and a peptide segment of the II–III loop of the dihydropyridine receptor. *J. Biol. Chem.* 274:7879–7886.
7. Casarotto, M. G., D. Green, S. M. Pace, S. M. Curtis, and A. F. Dulhunty. 2001. Structural determinants for activation or inhibition of ryanodine receptors by basic residues in the dihydropyridine receptor II–III loop. *Biophys. J.* 80:2715–2726.
8. Stange, M., A. Tripathy, and G. Meissner. 2001. Two domains in dihydropyridine receptor activate the skeletal muscle Ca^{2+} release channel. *Biophys. J.* 81:1419–1429.
9. O'Reilly, F. M., M. Robert, I. Jona, C. Szegedi, M. Albrieux, S. Geib, M. De Waard, M. Villaz, and M. Ronjat. 2002. FKBP12 modulation of the binding of the skeletal ryanodine receptor onto the II–III loop of the dihydropyridine receptor. *Biophys. J.* 82:145–155.
10. Proenza, C., C. M. Wilkens, and K. G. Beam. 2000. Excitation-contraction coupling is not affected by scrambled sequence in residues 681–690 of the dihydropyridine receptor II–III loop. *J. Biol. Chem.* 275:29935–29937.
11. Ahern, C. A., D. Bhattacharya, L. Mortenson, and R. Coronado. 2001. A component of excitation-contraction coupling triggered in the absence of the T671–L690 and L720–Q765 regions of the II–III loop of the dihydropyridine receptor α_{1s} pore subunit. *Biophys. J.* 81:3294–3307.
12. Wilkens, C. M., N. Kasielke, B. E. Flucher, K. G. Beam, and M. Grabner. 2001. Excitation-contraction coupling is unaffected by drastic alteration of the sequence surrounding residues L720–L764 of the α_{1S} II–III loop. *Proc. Natl. Acad. Sci. USA*. 98:5892–5897.
13. Fajloun, Z., R. Kharrat, L. Chen, C. Lecomte, E. Di Luccio, D. Bichet, M. El Ayeb, H. Rochat, P. D. Allen, I. N. Pessah, M. De Waard, and J. M. Sabatier. 2000. Chemical synthesis and characterization of maurocalcine, a scorpion toxin that activates Ca^{2+} release channel/ryanodine receptors. *FEBS Lett.* 469:179–185.
14. Esteve, E., S. Smida-Rezgui, S. Sarkozi, C. Szegedi, I. Regaya, L. Chen, X. Altafaj, H. Rochat, P. Allen, I. N. Pessah, I. Marty, J. M. Sabatier, I. Jona, M. De Waard, and M. Ronjat. 2003. Critical amino acid residues determine the binding affinity and the Ca^{2+} release efficacy of maurocalcine in skeletal muscle cells. *J. Biol. Chem.* 278: 37822–37831.
15. Lee, C. W., E. H. Lee, K. Takeuchi, H. Takahashi, L. Shimada, K. Sato, S. Y. Shin, D. H. Kim, and J. I. Kim. 2004. Molecular basis of the high-affinity activation of type 1 ryanodine receptors by imperatoxin A. *Biochem. J.* 377:385–394.
16. El-Hayek, R., A. J. Lokuta, C. Arevalo, and H. H. Valdivia. 1995b. Peptide probe of ryanodine receptor function. Imperatoxin A, a peptide from the venom of the scorpion *Pandinus imperator*, selectively activates skeletal-type ryanodine receptor isoforms. *J. Biol. Chem.* 270:28696–28704.
17. Tripathy, A., W. Resch, L. Xu, H. H. Valdivia, and G. Meissner. 1998. Imperatoxin A induces subconductance states in Ca^{2+} release channels (ryanodine receptors) of cardiac and skeletal muscle. *J. Gen. Physiol.* 111:679–690.
18. Shtifman, A., C. W. Ward, J. Wang, H. H. Valdivia, and M. F. Schneider. 2000. Effects of imperatoxin A on local sarcoplasmic reticulum Ca^{2+} release in frog skeletal muscle. *Biophys. J.* 79:814–827.
19. Szappanos, H., S. Smida-Resgui, J. Cseri, C. Simut, J. M. Sabatier, M. De Waard, L. Kovacs, L. Csernoch, and M. Ronjat. 2005. Differential effects of maurocalcine on Ca^{2+} release events and depolarization-induced Ca^{2+} release in rat skeletal muscle. *J. Physiol.* 565:843–853.
20. Altafaj, X., W. Cheng, E. Esteve, J. Urbani, D. Grunwald, J. M. Sabatier, R. Coronado, M. De Waard, and M. Ronjat. 2005. Maurocalcine and domain A of the II–III loop of the dihydropyridine receptor Cav 1.1 subunit share common binding sites on the skeletal ryanodine receptor. *J. Biol. Chem.* 280:4013–4016.
21. Jacquemond, V. 1997. Indo-1 fluorescence signals elicited by membrane depolarization in enzymatically isolated mouse skeletal muscle fibers. *Biophys. J.* 73:920–928.
22. Collet, C., B. Allard, Y. Tourneur, and V. Jacquemond. 1999. Intracellular calcium signals measured with indo-1 in isolated skeletal muscle fibres from control and mdx mice. *J. Physiol.* 520:417–429.
23. Collet, C., and V. Jacquemond. 2002. Sustained release of calcium elicited by membrane depolarization in ryanodine-injected mouse skeletal muscle fibers. *Biophys. J.* 82:1509–1523.
24. Collet, C., S. Pouvreau, L. Csernoch, B. Allard, and V. Jacquemond. 2004. Calcium signaling in isolated skeletal muscle fibers investigated under ''silicone voltage-clamp'' conditions. *Cell Biochem. Biophys.* 40:225–236.
25. Csernoch, L., J. C. Bernengo, P. Szentesi, and V. Jacquemond. 1998. Measurements of intracellular Mg^{2+} concentration in mouse skeletal muscle fibers with the fluorescent indicator mag-indo-1. *Biophys. J.* 75:957–967.
26. Pouvreau, S., B. Allard, C. Berthier, and V. Jacquemond. 2004. Control of intracellular calcium in the presence of nitric oxide donors in isolated skeletal muscle fibres from mouse. *J. Physiol.* 560:779–794.
27. Baylor, S. M., W. K. Chandler, and M. W. Marshall. 1983. Sarcoplasmic reticulum calcium release in frog skeletal muscle fibres estimated from Arsenazo III calcium transients. *J. Physiol.* 344: 625–666.
28. Timmer, J., T. Muller, and W. Melzer. 1998. Numerical methods to determine calcium release flux from calcium transients in muscle cells. *Biophys. J.* 74:1694–1707.
29. Chen, L., E. Esteve, J. M. Sabatier, M. Ronjat, M. De Waard, P. D. Allen, and I. N. Pessah. 2003. Maurocalcine and peptide A stabilize distinct subconductance states of ryanodine receptor type 1, revealing a proportional gating mechanism. *J. Biol. Chem.* 278:16095–16106.

30. Collet, C., L. Csernoch, and V. Jacquemond. 2003. Intramembrane charge movement and L-type calcium current in skeletal muscle fibers isolated from control and mdx mice. *Biophys. J.* 84:251–265.

31. Green, D., S. Pace, S. M. Curtis, M. Sakowska, G. D. Lamb, A. F. Dulhunty, and M. G. Casarotto. 2003. The three-dimensional structural surface of two β-sheet scorpion toxins mimics that of an α-helical dihydropyridine receptor segment. *Biochem. J.* 370:517–527.

32. Dulhunty, A. F., S. M. Curtis, S. Watson, L. Cengia, and M. G. Casarotto. 2004. Multiple actions of imperatoxin A on ryanodine receptors: interactions with the II–III loop ''A'' fragment. *J. Biol. Chem.* 279:11853–11862.

33. Lamb, G. D., R. El-Hayek, N. Ikemoto, and D. G. Stephenson. 2000. Effect of dihydropyridine receptor II–III loop peptides on Ca^{2+} release in skinned skeletal muscle fibers. *Am. J. Physiol.* 279: C891–C905.

34. Jacquemond, V., and M. F. Schneider. 1992. Low myoplasmic Mg^{2+} potentiates calcium release during depolarization of frog skeletal muscle fibers. *J. Gen. Physiol.* 100:137–154.